

Abundance and origin of fine particulate chloride in continental China

Xue Yang^{a, b}, Tao Wang^{b, a, *}, Men Xia^b, Xiaomen Gao^{a, d}, Qinyi Li^b, Naiwen Zhang^b, Yuan Gao^{b, e}, Shuncheng Lee^b, Xinfeng Wang^a, Likun Xue^a, Lingxiao Yang^{a, c}, Wenxing Wang^a

^a Environment Research Institute, Shandong University, Jinan, Shandong, China

^b Department of Civil and Environmental Engineering, The Hong Kong Polytechnic University, Hong Kong, China

^c School of Environmental Science and Engineering, Shandong University, Jinan, Shandong, China

^d School of Resources and Environment, University of Jinan, Jinan, Shandong, China

^e Department of Civil Engineering, the Chu Hai College of Higher Education, Castle Peak Bay, Hong Kong, China

* Corresponding author: Tao Wang (cetwang@polyu.edu.hk)

ABSTRACT

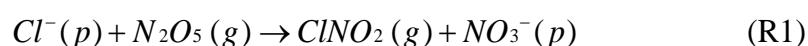
Particulate chloride can be converted to nitryl chloride (ClNO_2) through heterogeneous reactions with dinitrogen pentoxide (N_2O_5), and photolysis of ClNO_2 affects atmospheric oxidative capacity. However, the characteristics and sources of chloride, especially those with an anthropogenic origin, are poorly characterised, which makes it difficult to evaluate the effects of ClNO_2 on radical chemistry and air quality in polluted regions. Aerosol composition data from the literature were compiled to derive the spatial distributions of particulate chloride across China, and hourly aerosol composition data collected at a highly polluted inland urban site in eastern China and at a coastal site in southern China were analysed to gain further insights into non-oceanic sources of chloride. The results show that particulate chloride is concentrated mainly in fine particles and that high chloride loadings are observed in the inland urban areas of northern and western China with higher Cl^-/Na^+ mass ratios (2.46 to 5.00) than sea water (1.81), indicative of significant contributions from anthropogenic sources. At the inland urban site, the fine chloride displays distinct seasonality, with higher levels in winter and summer. Correlation analysis and positive matrix factorization (PMF) results indicate that coal combustion and residential biomass burning are the main sources (84.8%) of fine chloride in winter, and open biomass burning is the major source (52.7%) in summer. The transport of plumes from inland polluted areas leads to elevated fine chloride in coastal areas. A simulation with WRF-Chem model confirmed a minor contribution of sea-salt aerosol to fine chloride at the inland site during summer with winds from the East Sea. The widespread sources of chloride, together with abundant NO_x and ozone, suggest significant ClNO_2 production and subsequent enhanced photochemical processes over China.

Keywords: fine chloride; abundance; anthropogenic source; continental China

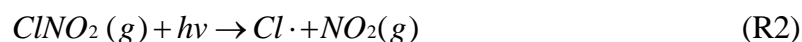
1. Introduction

Inorganic particulate chloride (Cl^-) has long been known to be an important component of aerosol in the maritime environment (O'Dowd and De Leeuw, 2007; Erickson and Duce, 1988). In recent years, it has attracted attention for its important roles in tropospheric chemistry (Faxon and Allen, 2013; Saiz-Lopez and von Glasow, 2012). Particulate chloride can be converted to nitryl chloride (ClNO_2) via heterogeneous reactions with dinitrogen pentoxide (N_2O_5) on aerosol surfaces at night

(Finlayson-Pitts et al., 1989).



ClNO₂ produced in the nocturnal reaction can release highly reactive chlorine radicals (Cl·) in the presence of sunlight (Riedel et al., 2012).



When present in the atmosphere, chlorine radicals play a crucial role in atmospheric photochemistry analogous to that of hydroxyl radicals (OH·), leading to the oxidation of volatile organic compounds and the formation of ozone (Knipping and Dabdub, 2003; Platt et al., 2004; Xue et al., 2015).

Generally, ClNO₂ production is controlled by chloride concentrations within particles and the availability of nitrogen oxides (NO_x = NO + NO₂) in the atmosphere. Previous studies indicated that the significant production of ClNO₂ usually occurs in near-coastal urban areas, where sea salt and NO_x sources coexist. For instance, chloride activation via ClNO₂ has been found on the Gulf Coast of the United States (Osthoff et al., 2008), in California (Riedel et al., 2012; Riedel et al., 2014) and in Hong Kong (Tham et al., 2014; Wang et al., 2016). However, high levels of ClNO₂ have also been observed in mid-continental regions removed from oceans, such as Weld County, Colorado (Riedel et al., 2013), southeast Texas (Faxon et al., 2015) and the North China Plain (Tham et al., 2016; Wang et al., 2014; Wang et al., 2017b). Thornton et al. (2010) found abundant chloride in fine aerosol and rainwater obtained from the national network of fine aerosol and precipitation in the United States. These studies demonstrate that a considerable amount of aerosol chloride is derived from non-marine sources that are able to sustain the production of ClNO₂ over large geophysical areas.

Particulate chloride in the boundary layer is generally considered to come from sea salts that mainly exist in coarse mode (aerodynamic diameter > 2.5 μm; PM_{2.5-10}), such as NaCl. Keene et al. (1999) estimated that globally, 99% of particulate chloride emission is from oceans. Particulate chloride also exists in fine mode (aerodynamic diameter <2.5 μm; PM_{2.5}) originating from various anthropogenic activities. For instance, industrial and power plant sources, such as coal combustion and manufacturing plants for hydrochloric acid, paper and chlorine-containing plastics emit chloride in industrial areas (Hara et al., 1989; McCulloch et al., 1999). Watson et al. (2001) detected significant emissions of laevoglucose, water soluble K⁺ and Cl⁻

during vegetative burning. [Pratt et al. \(2011\)](#) indicated that biomass burning is an important emission source of chloride, with particulate chloride existing primarily in the form of KCl. Forest fires, crop-stalk burning, residual wood combustion, and waste incineration emit not only carbonaceous aerosols but also sulphates, nitrates, chloride and potassium salts ([Clarke et al., 2011](#); [Hecobian et al., 2011](#); [Li et al., 2012](#)). Chloride observed in Toronto during winter has been attributed to the use of road salt ([Lee et al., 2003](#)).

Few studies have investigated the sources of chloride in ambient aerosols in mid-continental urban regions. [Mielke et al. \(2011\)](#) observed persistent ClNO₂ production (80 to 250 pptv) in Calgary, Canada, during April 2010 and attributed the aerosol chloride to the photolysis of anthropogenic Cl₂ and the suspension of road dust. [Jordan et al. \(2015\)](#) sampled bulk high-volume aerosol and size-segregated aerosols and suggested the contribution of soil dust to the observed particulate chloride in north-central Colorado via analysis of back trajectories, geographic information, size-resolved aerosol composition and elemental tracers. It is clear that the dominant sources of chloride vary among study areas.

Fast-paced industrialisation and urbanisation in China have led to severe atmospheric particulate matter (PM) pollution, and both PM₁₀ and PM_{2.5} levels frequently exceed the national ambient air quality standards ([Chan and Yao, 2008](#); [Yang et al., 2011](#)). NO_x and ozone pollution are also serious in major urban/industrial regions (e.g., [Wang et al., 2017a](#); [Xue et al., 2014](#)). Recent studies in southern and northern China revealed high mixing ratios of ClNO₂ (up to 4.7 ppb) associated with non-oceanic chloride ([Tham et al., 2016](#); [Wang et al., 2016](#); [Wang et al., 2017b](#); [Li et al., 2016](#)). To evaluate the production of ClNO₂ and its effects under high-aerosol loading and the high NO_x environment of China, it is important to understand the sources and abundance of the poorly characterised non-oceanic chloride. In this study, we reviewed hundreds of research reports on aerosol concentrations to obtain a general picture of the geographic distribution of chloride and to demonstrate the presence of significant non-oceanic sources in China. We then analysed 1-year measurements of chloride in PM_{2.5}, along with size-resolved distributions at an inland urban site in northern China and at a coastal site in southern China to shed light on the origins of fine particulate chloride. The results of this study improve our understanding of chloride production and emissions and the atmospheric impact of ClNO₂ in China.

2. Material and methods

2.1. Compilation of reported particulate chloride concentrations

In the recent years, chloride in $PM_{2.5}$ and PM_{10} at urban/non-urban areas in China has been widely measured and reported along with other major water-soluble ions (e.g., Cao et al., 2012; Chan and Yao, 2008; Yang et al., 2011). Most of these studies focused on major water-soluble ions such as SO_4^{2-} , NO_3^- and NH_4^+ because they make a significant contribution to the total mass of particulates. However, the sources of chloride have received little attention due to their relatively small contribution to total mass loading. In this study, we compiled the chloride data from published studies in internationally peer-reviewed journals. Among 130 publications that reported PM composition in China, 23 articles that presented Cl^- loadings in $PM_{2.5}$ are included in this paper (see Table A.1 in the Supplement). These 23 studies were conducted at 82 sites (60 urban and 22 non-urban sites) in 16 large cities (8 inland and 8 coastal; see Fig. 1) to derive the spatial distributions of particulate chloride across China. Four of the 23 articles also reported the level of Cl^- in PM_{10} , providing valuable information on the size distributions of chloride among the sites. To obtain the representative chloride level at a specific type of site in a particular city, the chloride value was averaged when there was more than one study.

2.2. Aerosol chloride content at one inland and one coastal site

The year-long ionic data, obtained from our previous field studies in Jinan and Tung Chung, Hong Kong, were analysed in this study to gain an understanding of the origins of particulate chloride in inland and coastal environments. These studies were conducted in Jinan from Dec 2007 to Oct 2008 and Tung Chung from Aug 2011 to May 2012. Wang et al. (2012) and Zhou et al. (2014) provide detailed descriptions of the sites, aerosol sampling and chemical analysis for the two sites, respectively. Briefly, Jinan is an inland city located in the centre of the North China Plain (Fig. 1). The field experiments were conducted on the campus of Shandong University (36°9'N, 117°06'E). The sampling site is surrounded by teaching, residential and commercial buildings. Tung Chung is a new town located in the west of Hong Kong. It receives air masses from the Pearl River Delta (PRD) and Hong Kong when northerly winds and easterly winds prevail, respectively (Gao et al., 2016; Xue et al., 2016).

The concentration of chloride in $PM_{2.5}$ and the size distribution of chloride were simultaneously measured at each site. Detailed information about measurement

techniques and quality control methods can be found elsewhere (Cao et al., 2012; Gao et al., 2016; Wang et al., 2012; Xu et al., 2011; Zhou et al., 2014). In brief, the concentration of chloride in $PM_{2.5}$ was continuously measured with an ambient ion monitor (AIM, Model 9000B, URG Corporation, USA). The size distribution of particulate chloride was obtained with a micro-orifice uniform deposit impactor (MOUDI, MSP, USA). Size-resolved aerosol samples were sampled every 3 to 7 days except for raining days. In total, data from 41 and 27 size-resolved particle sample days were obtained from Jinan and Tung Chung, respectively. Water soluble inorganic ions were analysed by ion chromatography (ICs-90, Dionex, USA).

Trace gases and meteorological parameters were concurrently measured at the two sites. CO was measured with a non-dispersive infrared analyser (Model 300E, API, USA), and SO₂ was measured with a pulsed UV fluorescence analyser (Model 43C, Thermo Electron Corporation, USA). Meteorological data including temperature (T), relative humidity (RH), and winds were obtained with automatic meteorological stations (PC-3 and PC-4, JZYG, China).

2.3. PMF model

Positive matrix factorization (PMF) was applied to apportion contributions to chloride in $PM_{2.5}$ from different emission sources. PMF is a factor-based receptor model based on multivariate statistical methods that decompose a matrix of sample data into matrices (US EPA, 2014). In this study, 245×11 matrix (sample number \times 11 species) and 793×9 matrix data sets were introduced to PMF 5.0 to identify chloride sources in Jinan in summer and winter, respectively. Note the inconformity of species number was due to instrument failure that resulted in the absence of corresponding data. The detailed model settings and physical parameterizations can be found in the user manual (US EPA, 2014) and related literature (Yang et al., 2013; Yao et al., 2016).

2.4. WRF-Chem model

An updated version of the Weather Research and Forecasting model coupled with Chemistry (WRF-Chem), incorporating the heterogeneous uptake process of nitrogen pentoxide (N₂O₅) and the subsequent production of nitryl chloride (ClNO₂) (Zhang et al., 2017) was used in this study to simulate the contribution of sea-salt aerosol to the levels of fine particulate chloride in the inland urban area. This model has been applied to investigate the impacts of heterogeneous uptake of dinitrogen

pentoxide (N_2O_5) and Cl activation and potential sources of nitrous acid (HONO) on ozone pollution (Zhang et al., 2017). In this study, the simulation domain covered eastern China and the adjacent oceanic areas with a grid resolution of 27 km. Sea-salt aerosol (Gong, 2003) was the sole chloride source considered in the simulation. The parameterisation options of the WRF model, such as anthropogenic and natural emissions, and meteorological and chemical simulations in the updated WRF-Chem follow those in Zhang et al. (2017).

3. Results and discussion

3.1. Chloride loadings in fine and coarse particles

The concentrations of chloride in $\text{PM}_{2.5}$ and PM_{10} , and the $\text{PM}_{2.5}/\text{PM}_{10}$ chloride ratios in seven areas are listed in Table 1 to identify the distribution of chloride loading in fine and coarse particles. It can be seen that the concentrations of chloride varied from 0.40 to 7.30 $\mu\text{g m}^{-3}$ for $\text{PM}_{2.5}$ and from 1.00 to 9.66 $\mu\text{g m}^{-3}$ for PM_{10} . The $\text{PM}_{2.5}/\text{PM}_{10}$ chloride ratios were greater than 0.6 in inland cities (e.g., Beijing, Nanjing) and in coastal cities during winter (e.g., Dalian, Qingdao, Guangzhou, Shenzhen and Hong Kong). In contrast, in summer, urban sites in the PRD, such as Guangzhou, Shenzhen and Hong Kong, showed relatively low (0.32 to 0.48) $\text{PM}_{2.5}/\text{PM}_{10}$ ratios, reflecting the increased influence of sea-salt aerosol during the summer monsoon (e.g., Wang et al., 2009).

Figure 2 further depicts the variations of chloride with particle size at the inland Jinan and coastal Tung Chung sites in different seasons. As shown, the patterns of chloride size distributions were consistent across the four seasons for each site but differed greatly between the two sites. Generally, three modes dominated the total mass distribution: a condensation mode (0.1 to 0.5 μm), a droplet mode (0.5 to 2 μm) and a coarse mode (2 to 50 μm). At the inland urban site, the chloride was concentrated in fine particles and peaked in the size range of 1.0 to 2.0 μm (i.e., the droplet mode), which had the largest mass fraction of the total suspended particulate (TSP; 47%), followed by the coarse mode (28%) and the condensation mode (25%). At the coastal site, the chloride concentration exhibited sharp peaks in the coarse mode that accounted for approximately 81% of the TSP. Compared with the coastal environment, the inland chloride was mostly concentrated in fine particles, and the detailed signature of the fine chloride that underlies this finding should be further explored.

3.2. Spatial distributions of fine chloride across China

Based on the 23 studies carried out in 16 large cities in China, the levels of chloride in PM_{2.5} were assembled to obtain a general picture of the geographical distribution of chloride, shown in Fig. 3. Averaged chloride concentration, chloride percentage in PM_{2.5}, and mass ratio of chloride/sodium (i.e., Cl⁻/Na⁺) varied substantially over these 16 locations. There was a nearly seven-fold variation in the average chloride concentration (0.77 to 5.23 μg m⁻³) across the sites. The highest chloride level (5.23 μg m⁻³) occurred in Xi'an, the capital city of Shaanxi province. The lowest chloride concentration (0.77 μg m⁻³), appeared in Hong Kong, a coastal city, but this was still 2 to 7 times higher than the concentrations measured in other coastal regions (0.11 to 0.34 μg m⁻³), such as Yokohama (Khan et al., 2010) and Istanbul (Szigeti et al., 2013). Inspection of the spatial distributions clearly indicated that high chloride loadings were most common in northern and western China, where most cities had average chloride concentrations in excess of 2.30 μg m⁻³ (see Fig. 3). Note that the chloride loadings in inland regions (e.g., Beijing, Jinan, Xi'an and Chongqing) were significantly greater than those in coastal areas (e.g., Guangzhou, Shenzhen and Hong Kong). Although Shanghai is also near the coast, it showed a higher chloride abundance than the other coastal sites, which can be explained by the intensive industrial and commercial activities at this megacity.

The mass ratio of Cl⁻/Na⁺ can be used as an indicator of the relative contributions of natural sources (e.g., sea salt) or anthropogenic sources to chloride. Sea salt contains Cl⁻, which tends to be replaced by acidic compounds in the atmosphere and is thus subject to significant chloride depletion (McInnes et al., 1994; Yao et al., 2003). However, Na⁺ is a chemically conserved constituent of sea salt. Consequently, the ratio of Cl⁻ to Na⁺ in aged sea salt during the transport to inland regions is generally lower than that of sea water (1.81) (Goldberg, 1963). Inspection of Cl⁻/Na⁺ ratios in these 16 large cities clearly indicated that inland urban areas in northern and western China (e.g., Beijing, Chongqing and Jinan) exhibited high Cl⁻/Na⁺ mass ratios (from 2.46 to 5), which were 3 to 10 times those in the coastal cities Shenzhen, Guangzhou and Hong Kong. This result reveals the significant contributions from non-oceanic sources to atmospheric chloride in inland regions of China.

A further indication of anthropogenic sources of chloride can be seen by comparing data from urban and rural sites within a region. Figure 4 depicts the

variations of chloride concentrations at paired urban/non-urban sites in eight regions. The percentage of chloride in PM_{2.5} and the Cl⁻/Na⁺ mass ratio at the urban sites are almost all higher than those at non-urban sites in a given region, indicating the existence of significant anthropogenic chloride sources in urban areas. Note that Tai Cang, which is a semi-rural site near Shanghai, had a chloride concentration comparable to that of Shanghai, which can be attributed to the transport of pollutant plumes from urban Shanghai during the sampling period (Pathak et al., 2009; Xue et al., 2014). Overall, these results indicate the high chloride loadings in the urban areas of northern and western China and suggest the existence of significant anthropogenic sources of particulate chloride.

3.3. Sources of chloride based on real-time data

3.3.1. Primary emissions from coal combustions and biomass burning

Table 2 compares the levels of chloride in PM_{2.5} for one whole year and also in different seasons at the inland urban (Jinan) and coastal suburban (Tung Chung) site. At the inland site, the annual average Cl⁻ concentration of fine chloride was 3.85 µg m⁻³, which was more than sixfold of that measured at the coastal site (0.61 µg m⁻³). The maximum hourly fine chloride concentration (36.9 µg m⁻³), which is the highest value recorded in open publications in China, was measured on 19 December, 2007. The concentrations of chloride at the inland urban site showed a clear seasonal pattern with 8.98 µg m⁻³ in winter, 3.25 µg m⁻³ in summer, 1.77 µg m⁻³ in spring and 1.41 µg m⁻³ in autumn. The concentrations of chloride at the coastal site showed much smaller seasonal changes with slightly higher levels in autumn.

To investigate the origins of high chloride loadings in the urban inland regions, the correlation coefficients between chloride and other major ions (NO₃⁻, SO₄²⁻, Na⁺, NH₄⁺, K⁺, Mg²⁺ and Ca²⁺) in different seasons were calculated for the urban Jinan site (see Table 3). The results show weak correlations between chloride and other ions in spring and autumn. In comparison, the winter chloride was correlated strongly with secondary formed ions (SO₄²⁻, NH₄⁺) and primary emission of Na⁺ and K⁺. SO₂ (hence SO₄²⁻) comes mainly from coal burning, whilst fine potassium (or K⁺/SO₄²⁻ ratio) has been extensively used as an indicator of biomass burning (Ma et al., 2003; Pratt et al., 2004; Wang et al., 2004; Zhou et al., 2010). Note that although Cl⁻ and Na⁺ were well correlated in Jinan in winter, the influence of sea salt would be minimal because the air masses generally come from the inland northwest in winter (Xu et al.,

2011), suggesting contributions of primary emissions from coal and biomass burning to the high concentrations of chloride in Jinan in winter. Figure 5a shows an example of such influence in a time series of the concentrations of chloride and related chemical tracers from 2 to 28 December 2007. The chloride sustained high levels that frequently exceeded $15 \mu\text{g m}^{-3}$ with high levels of SO_4^{2-} and elevated $\text{K}^+/\text{SO}_4^{2-}$ ratios. The chloride concentrations were correlated and increased positively with the SO_4^{2-} concentration ($r = 0.72$, see Fig. 5b), indicating that the abundant chloride mainly came from coal combustion. Indeed, in winter, large amounts of coal are burned to heat homes in both urban and rural areas of northern China. The chloride concentration also tracked with that of $\text{K}^+/\text{SO}_4^{2-}$, pointing to the potential influence of biomass burning. However, there were no fire spots over central-eastern China from 2 to 28 December 2007 according to satellite data (<http://firefly.geog.umd.edu/firemap/>), as shown in Fig. 5c. Hence, we suggest that residential biofuel combustion could be the reason for the high levels of chloride and potassium.

Furthermore, the PMF model was used to quantitatively identify the contributions of different sources to ambient chloride. Four resolved source profiles for chloride and related ions in $\text{PM}_{2.5}$ in winter are shown in Fig. 7a. The first factor was characterized by high amounts of Na^+ and Mg^{2+} , suggesting its relation to sea salt. The high loadings of Ca^{2+} combined with Mg^{2+} and Cl^- indicated that factor 2 was related to soil dust (Yang et al., 2013). As to the third factor, the secondary formation source was distinguished by high amounts of secondary formed ions, i.e., NO_3^- and NH_4^+ . Finally, based on the high SO_4^{2-} and K^+ levels, which were important markers for coal and biomass burning, representatively (Ma et al., 2003; Pratt et al., 2004), factor 4 was identified as coal and biomass burning. Obviously, among these four sources, coal and biomass combustion contributed most (as high as 84.8%) to the particulate chloride, followed by the soil dust (15.2%). Therefore, we interpreted the above results as evidence of significant contributions of coal burning and residential biomass combustion to the high abundance of chloride in winter in Jinan.

During summer, the fine chloride was well correlated ($r > 0.6$) with secondary formed ions (NH_4^+ , NO_3^-) and primary emission of K^+ (see Table 3), which can be interpreted as a strong contribution from the open-field burning of crop residues that has been observed in many field studies in northern and eastern China (e.g., Gao et al., 2012; Guo et al., 2004; Tham et al., 2016; Wang et al., 2002; Zhou et al., 2014). An examination of the summer data in Jinan revealed that high levels of chloride occurred

in the first part of the campaign, especially from 12 to 14 June 2008 (Fig. 6a). In the mornings of 12 to 14 June, the hourly concentration of fine chloride peaked above $6 \mu\text{g m}^{-3}$ and was well correlated with $\text{K}^+/\text{SO}_4^{2-}$ ratios ($r>0.8$; Figures not shown). Satellite data revealed concentrated fire dots south of Jinan, and backward trajectories originated from the southeast (Fig. 6b). The trajectories were calculated using the hybrid single-particle Lagrangian integrated model (HYSPLIT v4.9; Draxler and Rolph, 2016). These findings strongly suggest the influence of biomass burning on fine chloride measured in Jinan on 12 to 14 June 2008. Such inference is supported by the source profiles of chloride deduced from PMF analysis in summer of Jinan (see Fig. 7b). In summer in Jinan, totally five factors were identified for chloride, tracer gases and related ions in $\text{PM}_{2.5}$. Specifically, the first factor, recognized as secondary formation, was represented by secondary NO_3^- , SO_4^{2-} and NH_4^+ . The second factor was dominated by high loadings of SO_2 and SO_4^{2-} , which are typical species emitted from coal combustion. The third factor which could be attributed to soil dust had high levels of Ca^{2+} , Mg^{2+} and Na^+ . The fourth factor, characterized by high concentrations of F^- and a median load of Cl^- , was considered to be an industrial manufacture source. High concentration of F^- was generally linked to industrial manufactures including metal smelters and glass making (Pandey, 1981). The last factor was characterized by a relatively high load of Cl^- with a certain amount of K^+ , which is confirmed to be a unique biomass burning marker, indicating an origin of biomass burning (Ma et al., 2003). Of these five sources, only biomass burning and industrial manufacture contributed to the particulate chloride, with biomass burning being the major source contributor (52.7%). Therefore, based on the above correlation and PMF analysis, we conclude that the polluted air plume mixed with intensive biomass burning emissions contributed most to the high levels of chloride recorded in summer in Jinan.

3.3.2 Anthropogenic impact on chloride in coastal Hong Kong

Although summertime atmospheric chloride in Hong Kong mainly originated from sea salt associated with predominant winds from the oceans in summer, the influence of anthropogenic chloride sources can still be seen during pollution episodes when winds shifted to northerly. Figure 8a shows such a case depicting the time series of data collected at Tung Chung from 4 August to 7 September 2011. Severe aerosol (and ozone) pollution occurred from 25 to 31 August 2011 (Zhou et al., 2014; Xue et al., 2016). As shown in Fig. 8a, the concentrations of Cl^- , SO_4^{2-} , Na^+ , NH_4^+ , K^+ and

SO₂ were lower before August 24, which is consistent with back trajectories indicating winds from above oceans (Fig. 8b). Then, when winds shifted to northerly from the inland PRD, a significant increase in chloride and other species was observed with chloride reaching 0.44 μg m⁻³ in the early afternoon of 25 August, which was almost four times greater than the average summer chloride concentration of 0.11 μg m⁻³ in Tung Chung (see Table 2). A case captured during winter (1 to 3 March, 2013) also provides evidence of the important anthropogenic impact on chloride (see Fig. A.1). These findings demonstrate that even in coastal urban areas, the influence of anthropogenic sources can be significant.

3.4. The influence of sea salt in inland regions

As noted above, elevated levels of chloride have been observed in Jinan and other inland sites. The Jinan site is around 200 km from the nearest coast. In summer, dominant winds in the NCP are south-easterly (Gao et al., 2011), which may carry sea salt to inland regions. To quantify the potential influence of oceans on chloride, an updated WRF-Chem model (Zhang et al., 2017) was used to calculate the concentrations of Cl⁻ and Na⁺ in eastern China on 10 to 16 June 2008, when high levels of Cl⁻ and Na⁺ were simultaneously observed at the Jinan site (see Fig. 6a-c). We simulated both fine and coarse chloride with an assumption of emission from oceans being the sole chloride source.

Figure 9 shows model-simulated spatial distributions of average values of Cl⁻, Na⁺ and Cl⁻/Na⁺ mass ratios from 10 to 16 June 2008. It is apparent that both coarse mode Cl⁻ and Na⁺ from sea spray are concentrated in coastal regions and make a limited contribution to inland regions due to quick deposition (Sander et al., 2013). The simulated Cl⁻/Na⁺ mass ratios in fine aerosols are comparable to those in coarse aerosols in coastal regions, but much higher than those in coarse aerosols in inland regions. The simulated PM_{2.5} chloride concentration from sea salt was 0.25 μg m⁻³, much lower than the observed Cl⁻ concentration in Jinan (averaged value = 3.21 μg m⁻³ from 10 to 16 June 2008). This result indicates that sea salt makes a very limited contribution to the Jinan site and has an even smaller effect on areas further inland and confirms the existence of significant non-oceanic sources in large continental regions of China.

4. Conclusions

Based on aerosol composition data from the literature and our own observations,

the spatial distributions of particulate chloride across China and possible sources have been investigated. The results show that the particulate chloride was mainly concentrated in fine particles in inland areas. High chloride abundance and Cl^-/Na^+ mass ratios usually appeared in the cities in northern and western China, indicating the existence of non-oceanic chloride. At the inland urban site of Jinan, the fine chloride particles were at high levels and exhibited distinct seasonal variation, with the average chloride concentrations in winter and summer being higher than those in other seasons. Coal combustion and residential biomass burning contributed significantly (84.8%) to chloride in winter and open biomass burning contributed (52.7%) to the high levels of chloride in summer. The contribution of anthropogenic chloride is also evident in coastal Hong Kong when air masses come from inland China. WRF-Chem model calculations confirm the negligible contribution of sea salt to atmospheric chloride and the existence of strong anthropogenic chloride sources in inland areas. In view of the widespread chloride sources and the high levels of ozone and NO_x in urban regions of China, we propose that rapid chlorine activation and enhanced oxidation by chlorine radicals may occur in these regions, and we suggest that an accurate chloride emission inventory for China, which currently does not exist, should be developed to evaluate the effects of chlorine's action on ozone and haze pollution in China.

Acknowledgements

We thank Steven Poon, Wei Nie, Rui Gao, Zheng Xu, Shengzhen Zhou, Chao Yuan and Qiaozhi Zha for their help during the field measurements. We thank NOAA Air Resources Laboratory for the provision of the HYSPLIT model. Fire detection data was provided by <http://maps.geog.umd.edu/firms/>. This work was funded by the Hong Kong Research Grant Council (project C5022-14G), the National Natural Science Foundation of China (NSFC; 91544213) and the Hong Kong Polytechnic University (1-ZE13).

References

- Cao, J.J., Shen, Z.X., Chow, J.C., Watson, J.G., Lee, S.C., Tie, X.X., Ho, K.F., Wang, G.H., Han, Y.M., 2012. [Winter and summer \$\text{PM}_{2.5}\$ chemical compositions in fourteen Chinese cities. J. Air. Waste. Manage. Assoc. 62, 1214-1226.](#)
- Chan, C.K., Yao, X., 2008. [Air pollution in mega cities in China. Atmos. Environ. 42, 1-42.](#)
- Clarke, S., Eng, P., Preto, F., 2011. Biomass burn characteristics. [Ontario Ministry of Agriculture, Food, and Rural Affairs. Retrieved from](#)

<http://www.omafra.gov.on.ca/english/engineer/facts/11-033.pdf>.

- Draxler, R.R., Rolph, G.D., 2016. HYSPLIT (hybrid single particle Lagrangian integrated trajectory) model, NOAA Air Resource Laboratory, Silver Spring, MD. Accessed via <http://ready.arl.noaa.gov/HYSPLIT.php>.
- Erickson, D.J., Duce, R.A., 1988. On the global flux of atmospheric sea salt. *J. Geophys. Res.* 93, 14079-14088.
- Faxon, C.B., Allen, D.T., 2013. Chlorine chemistry in urban atmospheres: A review. *Environ. Chem.* 10, 221-233.
- Faxon, C.B., Bean, J.K., Ruiz, L.H., 2015. Inland concentrations of Cl₂ and ClNO₂ in southeast Texas suggest chlorine chemistry significantly contributes to atmospheric reactivity. *Atmosphere* 6, 1487-1506.
- Finlayson-Pitts, B., Ezell, M., Pitts, J., 1989. Formation of chemically active chlorine compounds by reactions of atmospheric NaCl particles with gaseous N₂O₅ and ClONO₂. *Nature* 337, 241-244.
- Gao, Y., Lee, S.C., Huang, Y., Chow, J.C., Watson, J.G., 2016. Chemical characterization and source apportionment of size-resolved particles in Hong Kong sub-urban area. *Atmos. Res.* 170, 112-122.
- Graedel, T.E., Keene, W., 1996. The budget and cycle of Earth's natural chlorine. *Pure Appl. Chem.* 68, 1689-1697.
- Goldberg, E.D., 1963. The oceans as a chemical system. In *The Sea*, Vol. II, ed. Hill, M.H. Interscience, London, pp. 3-26.
- Gong, S., 2003. A parameterization of sea-salt aerosol source function for sub - and super-micron particles. *Glob. Biogeochem. Cycles.* 17, 1097.
- Guo, H., Wang, T., Simpson, I.J., Blake, D.R., Yu, X.M., Kwok, Y.H., Li, Y.S., 2004. Source contributions to ambient VOCs and CO at a rural site in eastern China. *Atmos. Environ.* 38, 4551-4560.
- Hara, H., Kato, T., Matsushita, H., 1989. The mechanism of seasonal variation in the size distributions of atmospheric chloride and nitrate aerosol in Tokyo. *B. Chem. Soc. Jpn.* 62, 2643-2649.
- Hecobian, A., Liu, Z., Hennigan, C.J., Huey, L.G., Jimenez, J.L., Cubison, M.J., Vay, S., Diskin, G.S., Sachse, G.W., Wisthaler, A., Mikoviny, T., Weinheimer, A.J., Liao, J., Knapp, D.J., Wennberg, P.O., Kuerten, A., Crounse, J.D., St Clair, J., Wang, Y., Weber, R.J., 2011. Comparison of chemical characteristics of 495 biomass burning plumes intercepted by the NASA DC-8 aircraft during the ARCTAS/CARB-2008 field campaign. *Atmos. Chem. Phys.* 11, 13325-13337.
- Jordan, C., Pszenny, A., Keene, W., Cooper, O., Deegan, B., Maben, J., Routhier, M., Sander, R., Young, A., 2015. Origins of aerosol chlorine during winter over north central Colorado, USA. *J. Geophys. Res. Atmos.* 120, 678-694.
- Keene, W.C., Khalil, M.A.K., Erickson, D.J., McCulloch, A., Graedel, T.E., Lobert, J.M., Aucott, M.L., Gong, S.L., Harper, D.B., Kleiman, G., Midgley, P., Moore, R.M., Seuzaret, C., Sturges, W.T., Benkovitz, C.M., Koropalov, V., Barrie, L.A., Li, Y.F., 1999. Composite global emissions of reactive chlorine from anthropogenic and natural sources: Reactive chlorine emissions inventory. *J. Geophys. Res. Atmos.* 104, 8429-8440.
- Khan, M.F., Shirasuna, Y., Hirano, K., Masunaga, S., 2010. Characterization of PM_{2.5}, PM_{2.5-10} and PM_{>10} in ambient air, Yokohama, Japan. *Atmos. Res.* 96, 159-172.
- Knipping, E.M., Dabdub, D., 2003. Impact of chlorine emissions from sea-salt aerosol on coastal urban ozone. *Environ. Sci. Technol.* 37, 275-284.

- Lai, S.C., Zou, S.C., Cao, J.J., Lee, S.C., Ho, K.F., 2007. Characterizing ionic species in PM_{2.5} and PM₁₀ in four Pearl River Delta cities, South China. *J. Environ. Sci.* 19, 939-947.
- Lee, P.K., Brook, J.R., Dabek-Zlotorzynska, E., Mabury, S.A., 2003. Identification of the major sources contributing to PM_{2.5} observed in Toronto. *Environ. Sci. Technol.* 37, 4831-4840.
- Li, G., Lei, W., Bei, N., Molina, L.T., 2012. Contribution of garbage burning to chloride and PM_{2.5} in Mexico City. *Atmos. Chem. Phys.* 12, 8751-8761.
- Li, Q., Zhang, L., Wang, T., Tham, Y.J., Ahmadov, R., Xue, L., Zhang, Q., Zheng, J., 2016. Impacts of heterogeneous uptake of dinitrogen pentoxide and chlorine activation on ozone and reactive nitrogen partitioning: improvement and application of the WRF-Chem model in southern China. *Atmos. Chem. Phys.* 16, 14875-14890.
- Ma, Y., Weber, R.J., Lee, Y.N., Orsini, D.A., Maxwell-Meier, K., Thornton, D.C., Bandy, A.R., Clarke, A.D., Blake, D.R., Sachse, G.W., Fuelberg, H.E., Kiley, C.M., Woo, J.H., Streets, D.G., Carmichael, G.R., 2003. Characteristics and influence of biosmoke on the fine-particle ionic composition measured in Asian outflow during the Transport and Chemical Evolution over the Pacific (TRACE-P) experiment. *J. Geophys. Res. Atmos.* 108, 8816.
- McCulloch, A., Aucott, M.L., Benkovitz, C.M., Graedel, T.E., Kleiman, G., Midgley, P.M., Li, Y.F., 1999. Global emissions of hydrogen chloride and chloromethane from coal combustion, incineration and industrial activities: Reactive chlorine emissions inventory. *J. Geophys. Res. Atmos.* 104, 8391-8403.
- McInnes, L., Covert, D., Quinn, P., Germani, M., 1994. Measurements of chloride depletion and sulfur enrichment in individual sea-salt particles collected from the remote marine boundary layer. *J. Geophys. Res. Atmos.* 99, 8257-8268.
- Mielke, L.H., Furgeson, A., Osthoff, H.D., 2011. Observation of ClNO₂ in a mid-continental urban environment. *Environ. Sci. Technol.* 45, 8889-8896.
- O'Dowd, C.D., De Leeuw, G., 2007. Marine aerosol production: A review of the current knowledge. *Philos. Trans. R. Soc., Ser. A.* 365, 1753-1774.
- Osthoff, H.D., Roberts, J.M., Ravishankara, A.R., Williams, E.J., Lerner, B.M., Sommariva, R., Bates, T.S., Coffman, D., Quinn, P.K., Dibb, J.E., Stark, H., Burkholder, J.B., Talukdar, R.K., Meagher, J., Fehsenfeld, F.C., Brown, S.S., 2008. High levels of nitryl chloride in the polluted subtropical marine boundary layer. *Nat. Geosci.* 1, 324-328.
- Pandey, G., 1981. A survey of fluoride pollution effects on the forest ecosystem around an aluminium factory in Mirzapur, UP, India. *Environ. Conserv.* 8, 131-137.
- Pathak, R.K., Wu, W.S., Wang, T., 2009. Summertime PM_{2.5} ionic species in four major cities of China: Nitrate formation in an ammonia-deficient atmosphere. *Atmos. Chem. Phys.* 9, 1711-1722.
- Platt, U., Allan, W., Lowe, D., 2004. Hemispheric average Cl atom concentration from 13 C/12 C ratios in atmospheric methane. *Atmos. Chem. Phys.* 4, 2393-2399.
- Pratt, K.A., Murphy, S.M., Subramanian, R., DeMott, P.J., Kok, G.L., Campos, T., Rogers, D.C., Prenni, A.J., Heymsfield, A.J., Seinfeld, J.H., Prather, K.A., 2011. Flight-based chemical characterization of biomass burning aerosols within two prescribed burn smoke plumes. *Atmos. Chem. Phys.* 11, 12549-12565.
- Riedel, T.P., Bertram, T.H., Crisp, T.A., Williams, E.J., Lerner, B.M., Vlasenko, A., Li, S.-M., Gilman, J., De Gouw, J., Bon, D.M., 2012. Nitryl chloride and molecular chlorine in the coastal marine boundary layer. *Environ. Sci. Technol.* 46,

10463-10470.

- Riedel, T.P., Wagner, N.L., Dubé W.P., Middlebrook, A.M., Young, C.J., Öztürk, F., Bahreini, R., VandenBoer, T.C., Wolfe, D.E., Williams, E.J., 2013. Chlorine activation within urban or power plant plumes: Vertically resolved ClNO₂ and Cl₂ measurements from a tall tower in a polluted continental setting. *J. Geophys. Res. Atmos.* 118, 8702-8715.
- Riedel, T.P., Wolfe, G.M., Danas, K.T., Gilman, J.B., Kuster, W.C., Bon, D.M., Vlasenko, A., Li, S.M., Williams, E.J., Lerner, B.M., Veres, P.R., Roberts, J.M., Holloway, J.S., Lefer, B., Brown, S.S., Thornton, J.A., 2014. An MCM modeling study of nitryl chloride (ClNO₂) impacts on oxidation, ozone production and nitrogen oxide partitioning in polluted continental outflow. *Atmos. Chem. Phys.* 14, 3789-3800.
- Saiz-Lopez, A., von Glasow, R., 2012. Reactive halogen chemistry in the troposphere. *Chem. Soc. Rev.* 41, 6448-6472.
- Sander, R., Pszenny, A., Keene, W., Crete, E., Deegan, B., Long, M., Maben, J., Young, A., 2013. Gas phase acid, ammonia and aerosol ionic and trace element concentrations at Cape Verde during the Reactive Halogens in the Marine Boundary Layer (RHAMBLE) 2007 intensive sampling period. *Earth Syst. Sci. Data.* 5, 385-392.
- Shen, J., Liu, X., Zhang, Y., Fangmeier, A., Goulding, K., Zhang, F., 2011. Atmospheric ammonia and particulate ammonium from agricultural sources in the North China Plain. *Atmos. Environ.* 45, 5033-5041.
- Sun, Y., Zhuang, G., Wang, Y., Han, L., Guo, J., Dan, M., Zhang, W., Wang, Z., Hao, Z., 2004. The air-borne particulate pollution in Beijing-concentration, composition, distribution and sources. *Atmos. Environ.* 38, 5991-6004.
- Szigeti, T., Mihucz, V.G., Óvári, M., Baysal, A., Atılgan, S., Akman, S., Záray, G., 2013. Chemical characterization of PM_{2.5} fractions of urban aerosol collected in Budapest and Istanbul. *Microchem. J.* 107, 86-94.
- Takami, A., Wang, W., Tang, D., Hatakeyama, S., 2006. Measurements of gas and aerosol for two weeks in northern China during the winter-spring period of 2000, 2001 and 2002. *Atmos. Res.* 82, 688-697.
- Tham, Y.J., Wang, Z., Li, Q., Yun, H., Wang, W., Wang, X., Xue, L., Lu, K., Ma, N., Bohn, B., Li, X., Kecorius, S., Groß, J., Shao, M., Wiedensohler, A., Zhang, Y., Wang, T., 2016. Significant concentrations of nitryl chloride sustained in the morning: Investigations of the causes and impacts on ozone production in a polluted region of northern China. *Atmos. Chem. Phys. Discuss.* 2016, 1-34.
- Tham, Y.J., Yan, C., Xue, L., Zha, Q., Wang, X., Wang, T., 2014. Presence of high nitryl chloride in Asian coastal environment and its impact on atmospheric photochemistry. *Chinese Sci. Bull.* 59, 356-359.
- Thornton, J.A., Kercher, J.P., Riedel, T.P., Wagner, N.L., Cozic, J., Holloway, J.S., Dube, W.P., Wolfe, G.M., Quinn, P.K., Middlebrook, A.M., Alexander, B., Brown, S.S., 2010. A large atomic chlorine source inferred from mid-continental reactive nitrogen chemistry. *Nature* 464, 271-274.
- US EPA, 2014. Positive Matrix Factorization (PMF) 5.0 Fundamentals & User Guide. Office of Research and Development.
- Wang, G., Wang, H., Yu, Y., Gao, S., Feng, J., Gao, S., Wang, L., 2003. Chemical characterization of water-soluble components of PM₁₀ and PM_{2.5} atmospheric aerosols in five locations of Nanjing, China. *Atmos. Environ.* 37, 2893-2902.
- Wang, T., 2002. Emission characteristics of CO, NO_x, SO₂ and indications of biomass burning observed at a rural site in eastern China. *J. Geophys. Res.* 107, 4157.

- Wang, T., Tham, Y.J., Xue, L., Li, Q., Zha, Q., Wang, Z., Poon, S.C.N., Dubé W.P., Blake, D.R., Louie, P.K.K., Luk, C.W.Y., Tsui, W., Brown, S.S., 2016. Observations of nitryl chloride and modeling its source and effect on ozone in the planetary boundary layer of southern China. *J. Geophys. Res. Atmos.* 121, 2476-2489.
- Wang, T., Wei, X., Ding, A., Poon, S.C., Lam, K., Li, Y., Chan, L., Anson, M., 2009. Increasing surface ozone concentrations in the background atmosphere of Southern China, 1994-2007. *Atmos. Chem. Phys.* 9, 6217-6227.
- Wang, T., Wong, C., Cheung, T., Blake, D., Arimoto, R., Baumann, K., Tang, J., Ding, G., Yu, X., Li, Y., 2004. Relationships of trace gases and aerosols and the emission characteristics at Lin'an, a rural site in eastern China, during spring 2001. *J. Geophys. Res. Atmos.* 109.
- Wang, T., Xue, L., Brimblecombe, P., Lam, Y.F., Li, L., Zhang, L., 2017a. Ozone pollution in China: A review of concentrations, meteorological influences, chemical precursors, and effects. *Sci. Total Environ.* 575, 1582-1596.
- Wang, X., Wang, H., Xue, L., Wang, T., Wang, L., Gu, R., Wang, W., Tham, Y., Wang, Z., Yang, L., Chen, J., Wang, W., 2017b. Observations of N_2O_5 and $ClNO_2$ at a polluted urban surface site in North China: High N_2O_5 uptake coefficients and low $ClNO_2$ product yields. *Atmos. Environ.* 156, 125-134.
- Wang, X., Wang, T., Yan, C., Tham, Y.J., Xue, L., Xu, Z., Zha, Q., 2014. Large daytime signals of N_2O_5 and NO_3 inferred at 62 amu in a TD-CIMS: Chemical interference or a real atmospheric phenomenon? *Atmos. Meas. Technol.* 7, 1-12.
- Wang, X., Wang, W., Yang, L., Gao, X., Nie, W., Yu, Y., Xu, P., Zhou, Y., Wang, Z., 2012. The secondary formation of inorganic aerosols in the droplet mode through heterogeneous aqueous reactions under haze conditions. *Atmos. Environ.* 63, 68-76.
- Watson, J.G., Chow, J.C., Houck, J.E., 2001. $PM_{2.5}$ chemical source profiles for vehicle exhaust, vegetative burning, geological material, and coal burning in northwestern Colorado during 1995. *Chemosphere.* 43, 1141-1151.
- Xu, P., Wang, W., Yang, L., Zhang, Q., Gao, R., Wang, X., Nie, W., Gao, X., 2011. Aerosol size distributions in urban Jinan: Seasonal characteristics and variations between weekdays and weekends in a heavily polluted atmosphere. *Environ. Monit. Assess.* 179, 443-456.
- Xue, L., Gu, R., Wang, T., Wang, X., Saunders, S., Blake, D., Louie, P.K.K., Luk, C.W.Y., Simpson, I., Xu, Z., Wang, Z., Gao, Y., Lee, S., Mellouki, A., Wang, W., 2016. Oxidative capacity and radical chemistry in the polluted atmosphere of Hong Kong and Pearl River Delta region: Analysis of a severe photochemical smog episode. *Atmos. Chem. Phys.* 16, 9891-9903.
- Xue, L., Saunders, S., Wang, T., Gao, R., Wang, X., Zhang, Q., Wang, W., 2015. Development of a chlorine chemistry module for the Master Chemical Mechanism, *Geosci. Model Dev.* 8, 3151-3162.
- Xue, L.K., Wang, T., Gao, J., Ding, A.J., Zhou, X.H., Blake, D.R., Wang, X.F., Saunders, S.M., Fan, S.J., Zuo, H.C., Zhang, Q.Z., Wang, W.X., 2014. Ground-level ozone in four Chinese cities: Precursors, regional transport and heterogeneous processes. *Atmos. Chem. Phys.* 14, 13175-13188.
- Yang, F., Tan, J., Zhao, Q., Du, Z., He, K., Ma, Y., Duan, F., Chen, G., Zhao, Q., 2011. Characteristics of $PM_{2.5}$ speciation in representative megacities and across China. *Atmos. Chem. Phys.* 11, 5207-5219.
- Yang, L., Cheng, S., Wang, X., Nie, W., Xu, P., Gao, X., Yuan, C., Wang, W., 2013. Source identification and health impact of $PM_{2.5}$ in a heavily polluted urban

- atmosphere in China. *Atmos. Environ.* 75, 265-269.
- Yao, L., Yang, L., Yuan, Q., Yan, C., Dong, C., Meng, C., Sui, X., Yang, F., Lu, Y., Wang, W., 2016. Sources apportionment of PM_{2.5} in a background site in the North China Plain. *Sci. Total. Environ.* 541, 590-598.
- Yao, X.H., Fang, M., Chan, C.K., 2003. The size dependence of chloride depletion in fine and coarse sea-salt particles. *Atmos. Environ.* 37, 743-751.
- Zhang, L., Li, Q., Wang, T., Ahmadov, R., Zhang, Q., Li, M., Lv, M., 2017. Combined impacts of nitrous acid and nitryl chloride on lower tropospheric ozone: New module development in WRF-Chem and application to China. *Atmos. Chem. Phys.* 17, 9733-9750.
- Zhou, S., Wang, T., Wang, Z., Li, W., Xu, Z., Wang, X., Yuan, C., Poon, C.N., Louie, P.K.K., Luk, C.W.Y., Wang, W., 2014. Photochemical evolution of organic aerosols observed in urban plumes from Hong Kong and the Pearl River Delta of China. *Atmos. Environ.* 88, 219-229.
- Zhou, Y., Wang, T., Gao, X., Xue, L., Wang, X., Wang, Z., Gao, J., Zhang, Q., Wang, W., 2010. Continuous observations of water-soluble ions in PM_{2.5} at Mount Tai (1534 m a.s.l.) in central-eastern China. *J. Atmos. Chem.* 64, 107-127.

Table 1 Chloride concentrations in PM_{2.5} and PM₁₀ at various locations across China.
(unit: $\mu\text{g m}^{-3}$)

Table 2 Seasonal variations of chloride, sodium, Cl^-/Na^+ ratios and Cl^- percentage in PM_{2.5} in Ji'nan and Tung Chung (unit: $\mu\text{g m}^{-3}$).

Table 3 Correlation coefficients (r) between chloride and other major ions in PM_{2.5} in spring, summer, autumn and winter in Ji'nan.

Table 1 Chloride concentrations in PM_{2.5} and PM₁₀ at various locations across China. (unit: $\mu\text{g m}^{-3}$)

Location	Type of site	Study period	PM _{2.5}			PM ₁₀			Cl ⁻ (PM _{2.5})/
			Cl ⁻	Cl%	Cl ⁻ /Na ⁺	Cl ⁻	Cl%	Cl ⁻ /Na ⁺	Cl ⁻ (PM ₁₀)
Beijing ^a	Urban	2002–2003 summer	1.69	2.24%	-	2.29	1.53%	-	0.74
	Urban	2002–2003 winter	7.36	4.04%	-	9.66	3.30%	-	0.76
	Suburban	Aug 2006 – Sep 2009	2.80	2.06%	-	3.70	1.81%	-	0.76
Dalian ^b	Urban	Feb–Mar 2002	1.96	2.90%	1.32	2.70	2.91%	1.29	0.73
Qingdao ^b	Urban	Feb–Mar 2001	0.96	1.70%	1.70	1.50	1.53%	1.50	0.64
Nanjing ^c	Urban	Feb–Dec 2001	1.08	0.34%	0.46	1.51	0.48%	0.40	0.72
	Urban	Jan–Feb 2002	2.70	2.98%	0.59	3.40	2.46%	0.63	0.79
Guangzhou ^d	Urban	Jun–Jul 2002	0.80	1.21%	0.23	2.50	2.43%	0.47	0.32
	Suburban	Jan–Feb 2002	6.30	4.55%	1.19	7.40	3.64%	1.37	0.85
	Suburban	Jun–Jul 2002	1.20	1.53%	0.32	2.50	1.93%	0.35	0.48
Shenzhen ^d	Urban	Jan–Feb 2002	2.10	3.45%	0.48	2.60	3.11%	0.47	0.81
	Urban	Jun–Jul 2002	1.00	2.12%	0.28	2.70	3.60%	0.49	0.37
Hong Kong ^d	Urban	Jan–Feb 2002	1.80	3.71%	0.38	2.10	3.77%	0.39	0.86
	Urban	Jun–Jul 2002	0.40	1.30%	0.13	1.00	2.59%	0.20	0.40

^a (Shen et al., 2011; Sun et al., 2004); ^b (Takami et al., 2006); ^c (Wang et al., 2003); ^d (Lai et al., 2007)

Table 2 Seasonal variations of chloride, sodium, Cl^-/Na^+ ratios and Cl^- percentage in $\text{PM}_{2.5}$ in Ji'nan and Tung Chung (unit: $\mu\text{g m}^{-3}$).

Ji'nan	Spring	Summer	Autumn	Winter	Annual
Cl^-	1.77	3.25	1.41	8.98	3.85
Na^+	0.86	2.49	1.04	1.31	1.43
Cl^-/Na^+	2.06	1.31	1.36	6.85	2.70
$\text{Cl}^- \%$	2.89	2.59	2.32	8.06	4.33
Tung Chung	Spring	Summer	Autumn	Winter	Annual
Cl^-	0.47	0.11	1.02	0.82	0.61
Na^+	0.63	0.37	0.66	0.90	0.64
Cl^-/Na^+	0.75	0.30	1.55	0.91	0.95
$\text{Cl}^- \%$	5.37	4.08	6.15	5.38	5.24

Table 3 Correlation coefficients (r) between chloride and other major ions in $\text{PM}_{2.5}$ in spring, summer, autumn and winter in Ji'nan.

Season		NO_3^-	SO_4^{2-}	Na^+	NH_4^+	K^+	Mg^{2+}	Ca^{2+}
Spring	Cl^-	0.18	0.21	0.45	-0.02	0.59	0.15	0.08
Summer	Cl^-	0.73	0.37	-0.07	0.67	0.61	0.49	0.57
Autumn	Cl^-	0.38	0.06	0.28	0.17	0.40	0.31	0.11
Winter	Cl^-	0.57	0.73	0.74	0.78	0.82	0.32	0.47

Figure Captions

Fig. 1. Left: Locations of the 16 large cities for which particulate chloride concentrations were measured and compiled in this study. Eight coastal cities are marked in red, and eight inland cities (at least 100 km from the nearest coastline) are marked in green. Right: locations of the sampling sites in Jinan and Hong Kong (Tung Chung).

Fig. 2. Average chloride concentration as a function of size from the MOUDI sampler in different seasons in Jinan and Tung Chung.

Fig. 3. Spatial distributions of chloride at urban locations in China. Average chloride concentration ($\mu\text{g m}^{-3}$), percentage of chloride in $\text{PM}_{2.5}$ ($\text{Cl}^- \%$) and Cl^-/Na^+ mass ratio are indicated. Inland and coastal cities are marked in green and red, respectively.

Fig. 4. Comparison of chloride concentration ($\mu\text{g m}^{-3}$), percentage of chloride in $\text{PM}_{2.5}$, $\text{Cl}^- \%$ and Cl^-/Na^+ mass ratio at paired urban/non-urban sites in representative cities.

Fig. 5. (a) Time series of air pollutants observed in winter in Jinan, (b) Scatter plot of Cl^- and SO_4^{2-} in winter and (c) corresponding fire counts over east-central China from Aqua and Terra MODIS.

Fig. 6. (a) Time series of air pollutants observed in summer in Jinan and corresponding fire counts over east-central China from Aqua and Terra MODIS: (b) 12 to 14 June 2008; (c) 15 to 16 June 2008.

Fig. 7. Source profiles of chloride and other tracer species deduced from PMF analysis in Jinan in (a) winter and (b) summer, respectively.

Fig. 8. (a) Time series of air pollutants observed in summer in Tung Chung; (b) Back trajectories before, during and after the episodic period (i.e., 25 to 31 August 2011) with colour showing the monthly mean OMI-derived NO_2 column density in August 2011 (<http://www.temis.nl/airpollution/no2.html>).

Fig. 9. WRF-Chem simulated spatial distributions of (a) fine mode Cl^- ($\mu\text{g m}^{-3}$), (b) coarse mode Cl^- ($\mu\text{g m}^{-3}$), (c) fine mode Na^+ ($\mu\text{g m}^{-3}$), (d) coarse mode Na^+ ($\mu\text{g m}^{-3}$), (e) mass ratios of fine $\text{Cl}^-/\text{fine Na}^+$ and (f) mass ratios of coarse $\text{Cl}^-/\text{coarse Na}^+$ in China from June 10 to 16 2008.

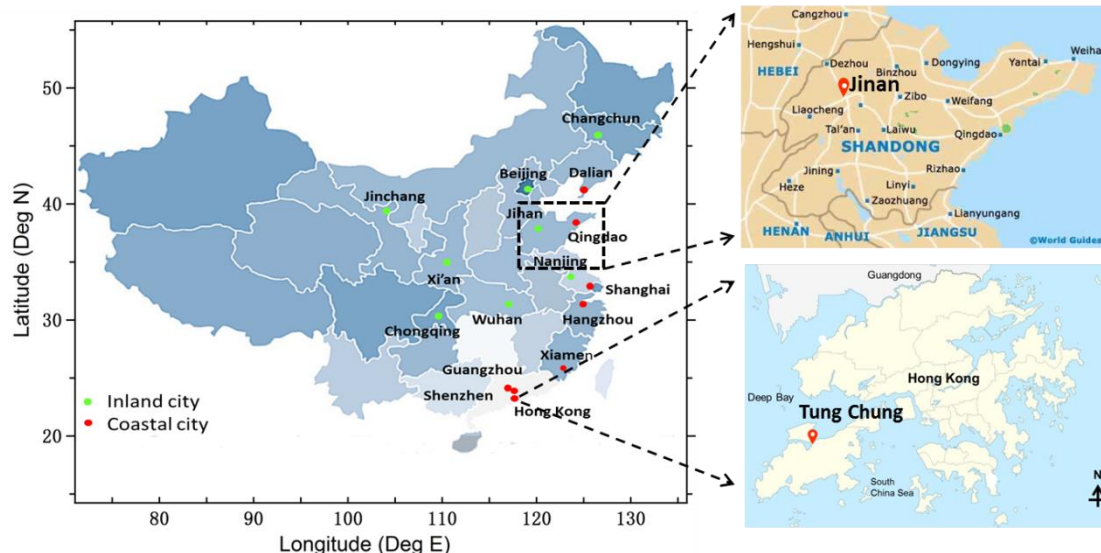


Fig. 1. Left: Locations of the 16 large cities for which particulate chloride concentrations were measured and compiled in this study. Eight coastal cities are marked in red, and eight inland cities (at least 100 km from the nearest coastline) are marked in green. Right: locations of the sampling sites in Jinan and Hong Kong (Tung Chung).

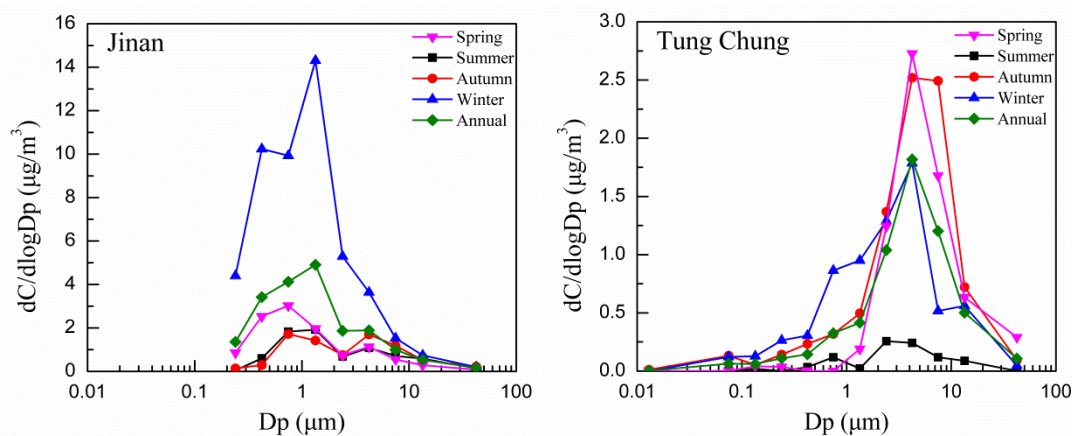


Fig. 2. Average chloride concentration as a function of size from the MOUDI sampler in different seasons in Jinan and Tung Chung.

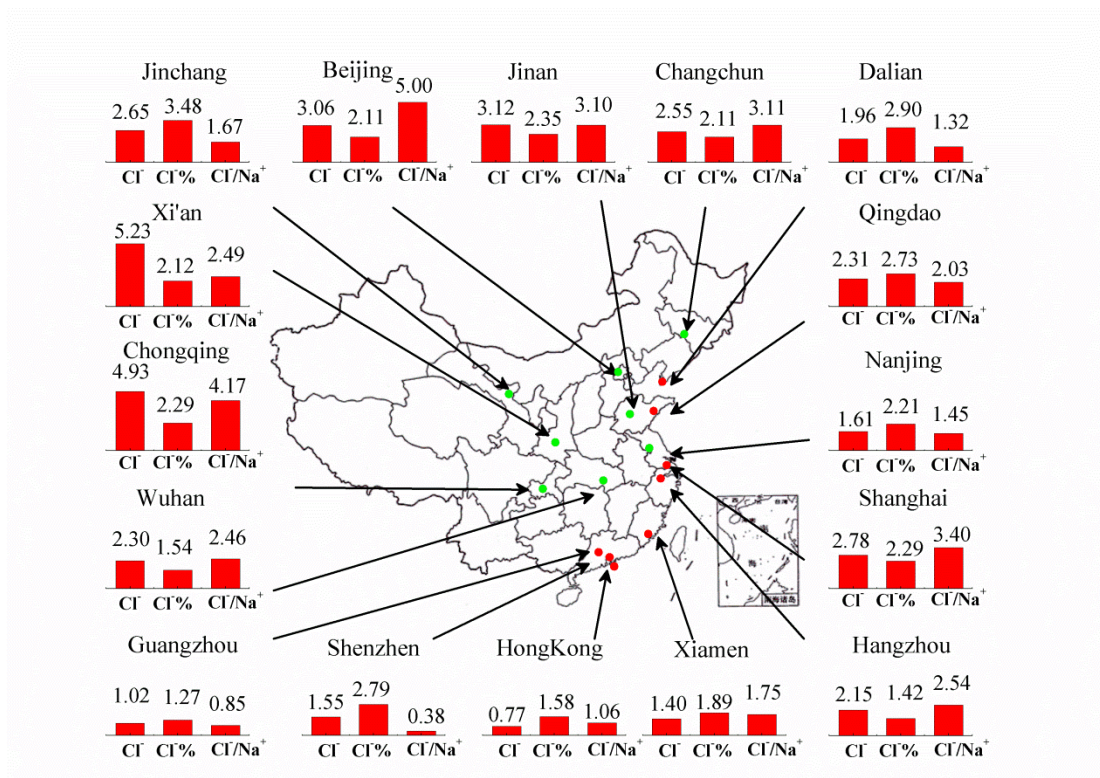


Fig. 3. Spatial distributions of chloride at urban locations in China. Average chloride concentration ($\mu\text{g m}^{-3}$), percentage of chloride in $\text{PM}_{2.5}$ ($\text{Cl}^- \%$) and Cl^-/Na^+ mass ratio are indicated. Inland and coastal cities are marked in green and red, respectively.

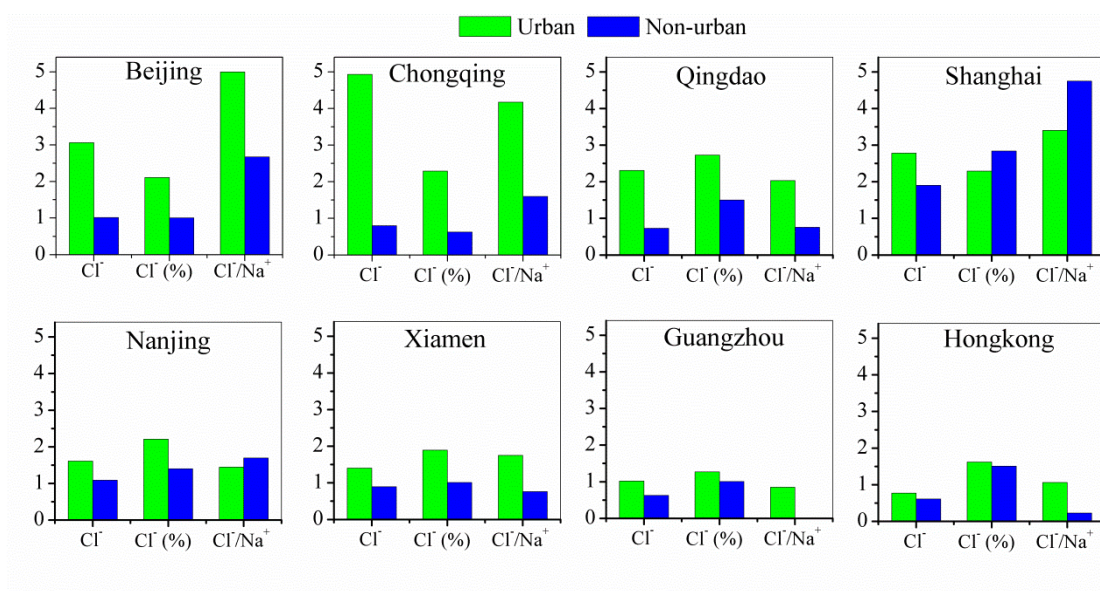


Fig. 4. Comparison of chloride concentration ($\mu\text{g m}^{-3}$), percentage of chloride in $\text{PM}_{2.5}$, $\text{Cl}^- \%$ and Cl^-/Na^+ mass ratio at paired urban/non-urban sites in representative cities.

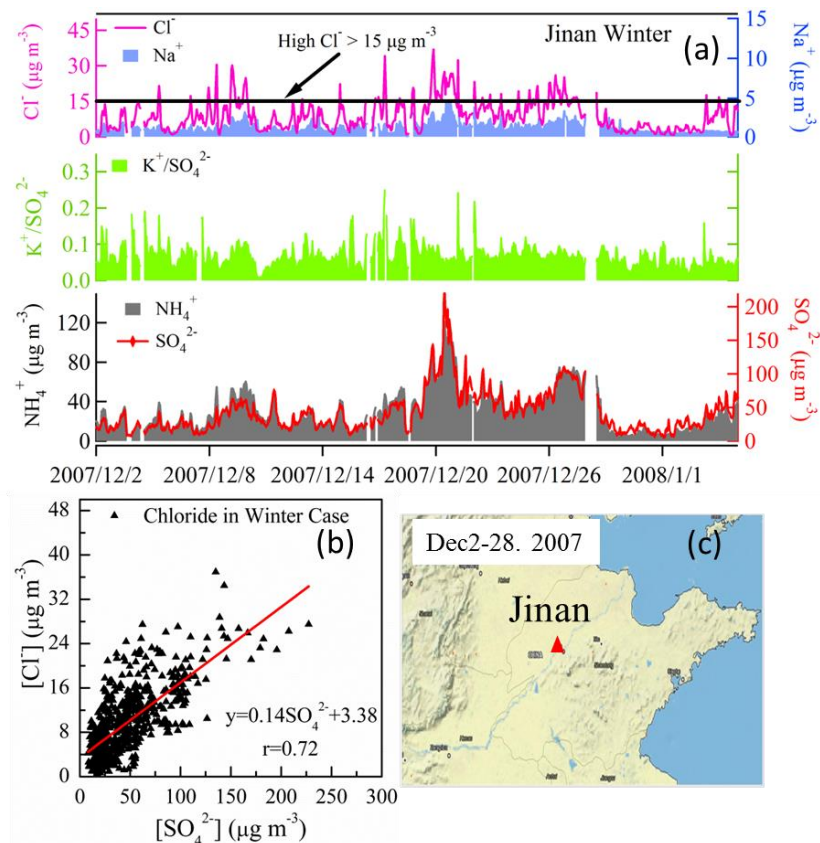


Fig. 5. (a) Time series of air pollutants observed in winter in Jinan, (b) Scatter plot of Cl^- and SO_4^{2-} in winter and (c) corresponding fire counts over east-central China from Aqua and Terra MODIS.

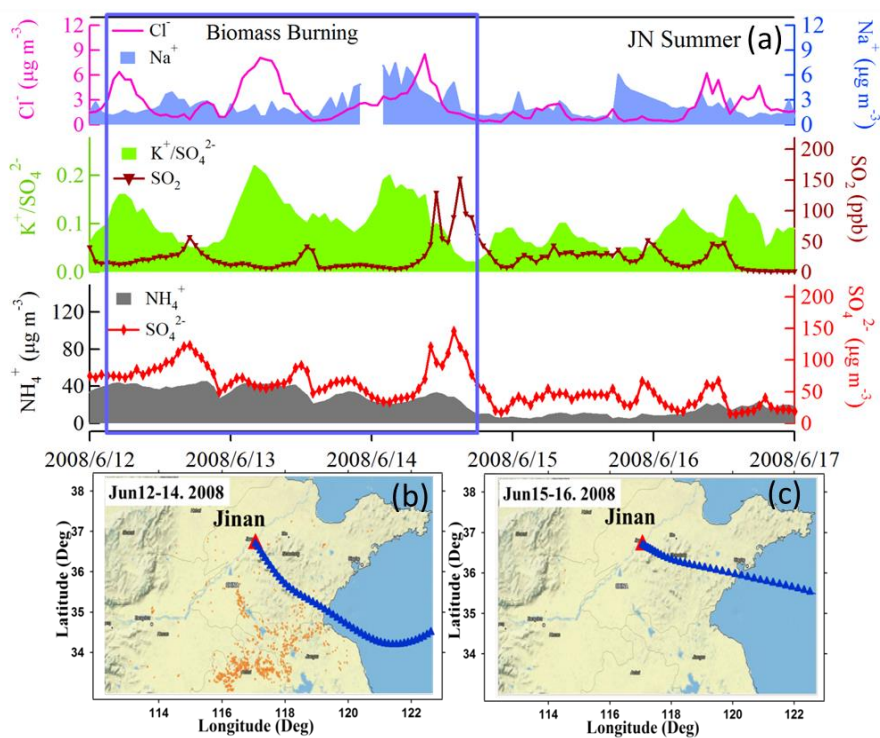


Fig. 6. (a) Time series of air pollutants observed in summer in Jinan and corresponding fire counts over east-central China from Aqua and Terra MODIS: (b) 12 to 14 June 2008; (c) 15 to 16 June 2008.

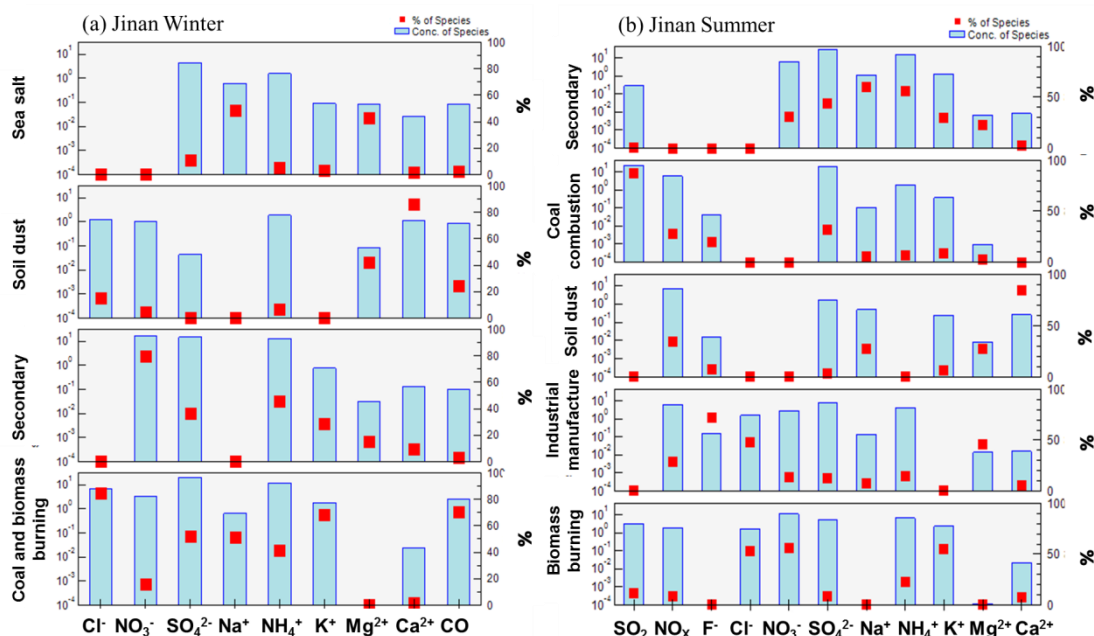


Fig. 7. Source profiles of chloride and other tracer species deduced from PMF analysis in Jinan in (a) winter and (b) summer, respectively.

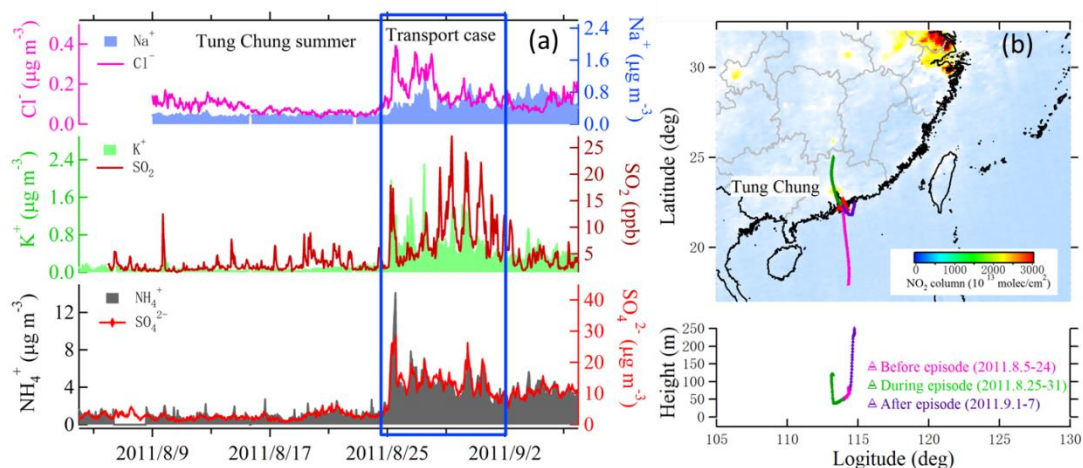


Fig. 8. (a) Time series of air pollutants observed in summer in Tung Chung; (b) Back trajectories before, during and after the episodic period (i.e., 25 to 31 August 2011) with colour showing the monthly mean OMI-derived NO_2 column density in August 2011 (<http://www.temis.nl/airpollution/no2.html>).

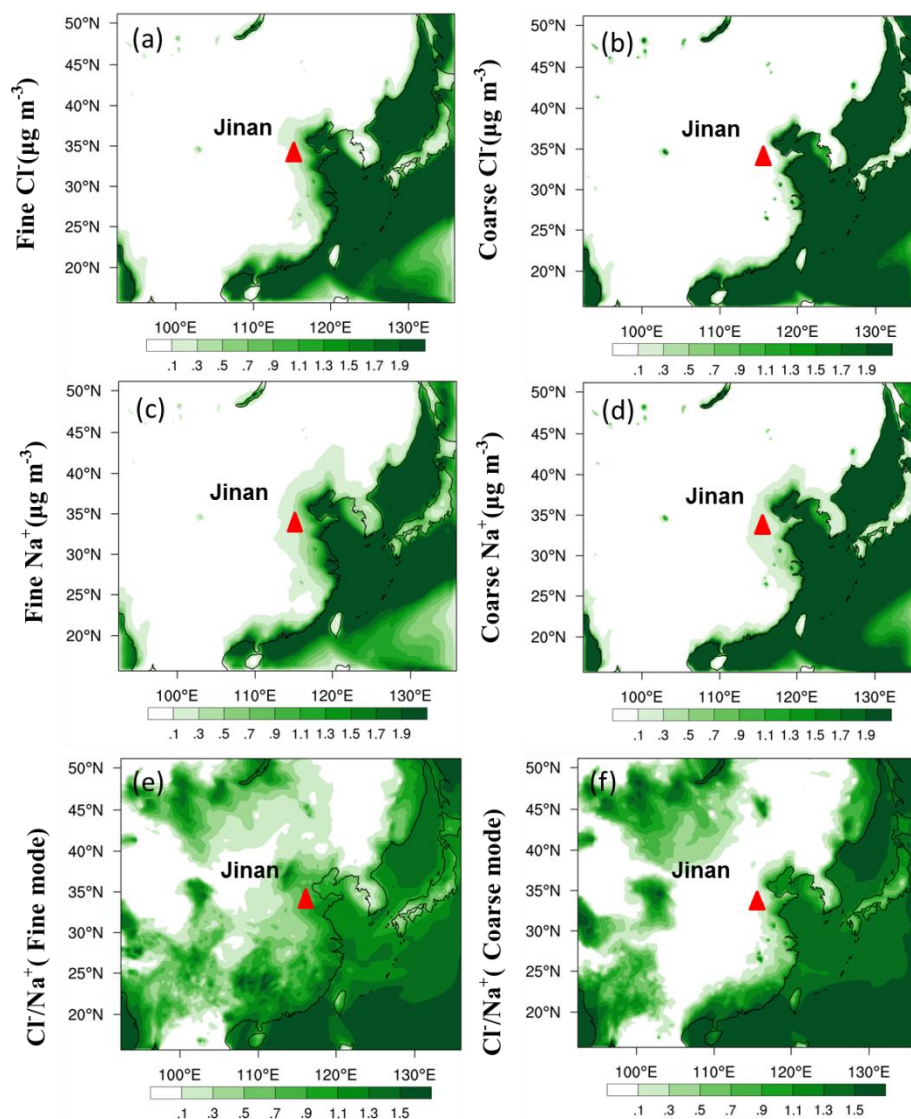


Fig. 9. WRF-Chem simulated spatial distributions of (a) fine mode Cl^- ($\mu\text{g m}^{-3}$), (b) coarse mode Cl^- ($\mu\text{g m}^{-3}$), (c) fine mode Na^+ ($\mu\text{g m}^{-3}$), (d) coarse mode Na^+ ($\mu\text{g m}^{-3}$), (e) mass ratios of fine Cl^-/Na^+ and (f) mass ratios of coarse Cl^-/Na^+ in China from June 10 to 16 2008.